DOI: 10.7795/810.20240208B

SPECTRAL DEPENDENT NON-LINEARITY OF CHARGE ACCUMULATING PIXEL MATRIX SENSORS

Christian Schrader, Johannes Ledig

Physikalisch-Technische Bundesanstalt, Braunschweig and Berlin, Germany

Acknowledgement: This project has received funding from the EMPIR programme co-financed by the Participating States and from the European Union's Horizon 2020 research and innovation programme.

SPECTRAL DEPENDENT NON-LINEARITY OF CHARGE ACCUMULATING PIXEL MATRIX SENSORS

Schrader, C.[1], Ledig, J.[1]
[1] Physikalisch-Technische Bundesanstalt, Braunschweig, GERMANY
christian.schrader@ptb.de

Abstract

The application of camera systems based on charge accumulating sensors for quantitative measurements of light distributions requires correction of significant systematic errors like non-linearity. A characteristic type of signal non-linearity that often occurs is a linear decreasing one. This contradicts the assumption of imperfections of the device to be the source of non-linearity but looks like a systematic effect. This work will describe the search for the reason of this type of non-linearity which ends in the observation of a spectral dependence of the non-linearity. A first approach to correct this effect without knowing the source spectrum is presented.

Keywords: Non-linearity, Pixel-Sensor, Camera, ILMD

1 Introduction

Camera systems based on charge accumulating pixel sensors (e. g. CCD, CMOS) are widely used to carry out quantitative measurements of light distributions, especially when used in imaging luminance measurement devices (ILMDs). To increase the accuracy of the absolute measurements these devices need to be characterized in a way that significant systematic effects can be corrected. One element of this characterization is the non-linearity of the system. The origins of the non-linearity are usually attributed to imperfect behaviour during charge transfer (for CCDs), amplification, sampling and AD-conversion which can be subsumed as signal processing in the Analog-Front-End (AFE) (Ferrero et al., 2006).

Under the precondition that no internal reconfiguration occurs (e.g. constant gain factors, bias voltage, offset voltage), the number of collected electrons can be seen as the internal quantity that defines the working point of this analogue signal processing chain. The number of collected electrons n_e is not accessible but it is directly linked to the output signal y by the internal system gain k_sys. Therefore, the non-linearity can also be modelled as a function of the output signal y, which is accessible. The non-linearity in this context is the change of the system gain relative to a reference value.

To determine the non-linearity, the range of accumulated electrons need to be changed from zero to the maximum possible number where y is not limited by the limit of the AD-converter (no clipping). This can be achieved by varying the integration time for a constant illumination or by varying the spectral irradiance on the sensor for constant integration time. In photometry, typically the radiation of a white light source, e.g. of a luminance standard, is used for measurement. The variation of the integration time is usually simpler to implement than a variation of the sensor's spectral irradiance with known irradiance ratios and constant spectral distribution. From the output signals y an offset value y_0 gets subtracted which results from an internal offset voltage added device-internally to the signal to prevent clipping of the dark signal including its noise during AD-conversion:

$$y_\mathrm{oc} = y - y_0 \tag{1}$$

For ideal systems the offset corrected signal y_oc is then proportional to the integration time t_int. Or, in other words, the signal rate

$$y_\mathrm{rate} = \frac{y_\mathrm{oc}}{t_\mathrm{int}} \tag{2}$$

corresponding to the photocurrent inside the pixel should be constant. To make the signal rate independent of the absolute pixel irradiance, all values of the signal rate series are normalized

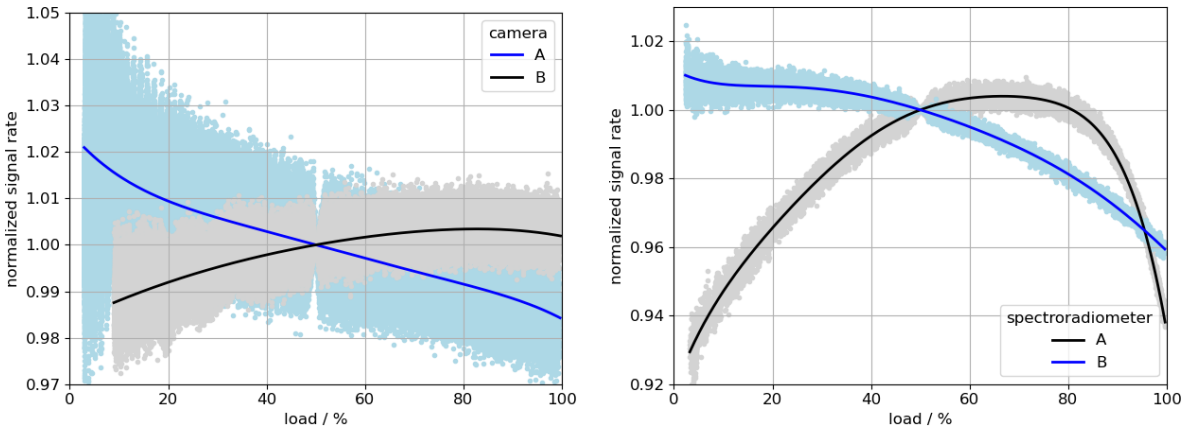

Figure 1 – Examples of non-linearity characteristics by normalized data points (light colour) and their polynomial representation (lines) for cameras (left) and spectroradiometers (right) based on charge accumulating pixel sensors

to a reference value, e.g. the interpolated value of this series at a given signal value or the average signal rate of the series.

$$y_{\mathrm{rate,rel}} = \frac{y_{\mathrm{rate}}(y_{\mathrm{oc}})}{y_{\mathrm{rate,ref}}} \tag{3}$$

The change of this normalized signal rate $y_{\mathrm{rate,rel}}$ represents the relative non-linearity of the signal-processing chain. When this is done for all pixels, it results in a cloud of data points which may be dominated by the photon noise. To separate the systematic non-linearity component from the noise component, a function $f_{\mathrm{NL,sigproc}}(\mathrm{y_{oc}})$ is fitted to the data points. This can be a polynomial, c-spline, or some other appropriate function type. For fast application a lookup table can be derived from this function. In this work we use a polynomial representation.

Because the precise value of the integration time is important for this calculation, the accuracy of its realisation is important. Therefore, it is recommended not to use very short integration times (usually below the milli-second regime) because there the uncertainty of their realisation can significantly influence the measured non-linearity. Additionally, namely for CCD sensors, the smear effect will increase the non-linearity at low output signals.

Figure 1 shows some examples of these normalized data points and the fitted polynomial (in the following images only the polynomial representations are plotted). The abscissa represents offset corrected signal values y_{oc}, as percentage to the available dynamic range (load) of the

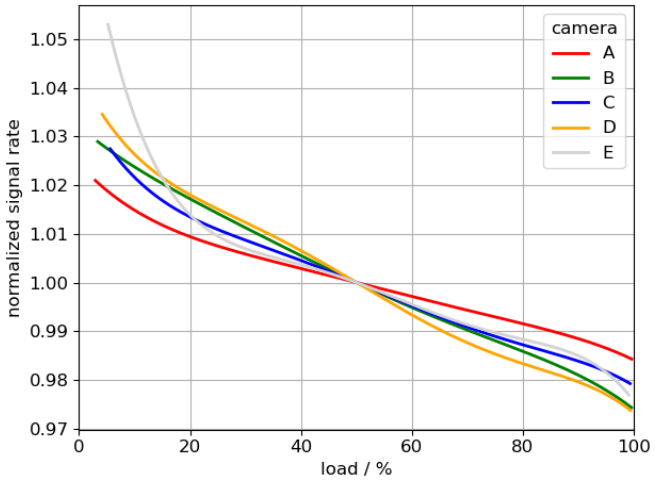

Figure 2 – Examples for “linear” non-linearity characteristics

AD converter margin above the offset ($y_{\mathrm{load\%}} = \frac{y_{\mathrm{oc}} \cdot 100}{y_{\mathrm{ADC,max}} - 1 - y_0}$). The resulting characteristics are somewhat curved in a range of a few percent which usually is a significant error. This corresponds to the understanding that the origin of the non-linearity are imperfections of the AFE. This characterisation was carried out by the authors for different camera systems and array spectroradiometers as part of their characterisation. During these characterisations one class of non-linearity characteristics showed up which are summarised for different devices in Figure 2.

All characteristics start at low signal levels with positive values and then go down nearly linear to high signal levels. This seems to be contradicting to the assumption to be based on imperfections of the AFE realization. The fact that this behaviour was seen on different devices (e.g. ILMDs and industrial cameras) lead to the assumption, that this is not just a shape reflecting random imperfections but that there must be another systematic effect that causes this behaviour. This work will discuss the search for the underlaying effect and its correction by post processing of the measurement signal.

2 Measurements

The goal is to identify an inner working principle that prefers low signal levels and suppresses higher ones. To do this, a set of measurements with special configuration or optical stimulus were carried out. Hereby usually only one camera was used, depending on which settings were available on which device.

Despite there was no suspected inner working principle affecting the full signal range, the first point to be checked was a dependence of the scene luminance and therefore the range of the used integration time to scan the load range. These measurements were done using an ILMD because it allows longer integration times than the industrial cameras designed for machine vision. The light source was a luminance standard based on an incandescent lamp. By adding neutral-density-(ND)-filters the luminance was reduced to achieve an integration time of 6 ms, 100 ms, and 5500 ms for full load. Figure 3 shows the measured non-linearities. The result shows no systematic dependence on the integration time for most of these measurements.

The next suspected effect was a dependence on the internal pixel clock. This defines the timing for the readout and analogue processing of the pixel signals. During readout the voltages of the pixel signals are multiplexed to one or more AD-converter. The slew rates might depend on the signal level and limit the establishment of a stationary voltage level between start of a voltage pulse and the moment of sampling. So, for larger pixel signal the relative error of the measurement of the corresponding voltage steps would get larger. To test this mechanism a machine vision camera (with CCD sensor) was used that allows the change of the internal pixel clock. If this mechanism would be effective, a change of the pixel clock should change the average slope

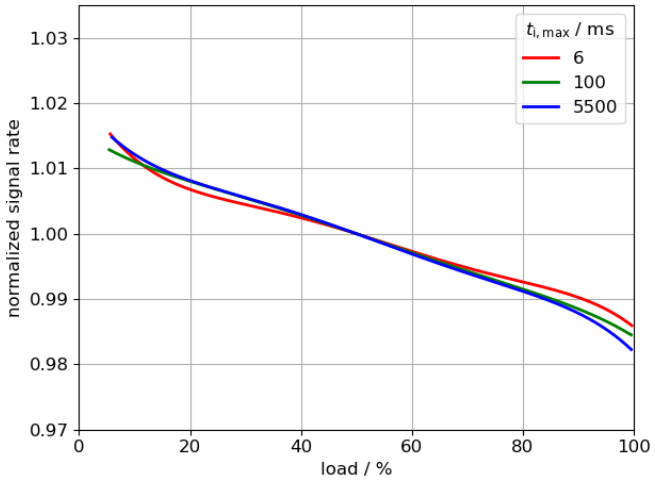

Figure 3 – Dependence of the non-linearity characteristic on the integration time

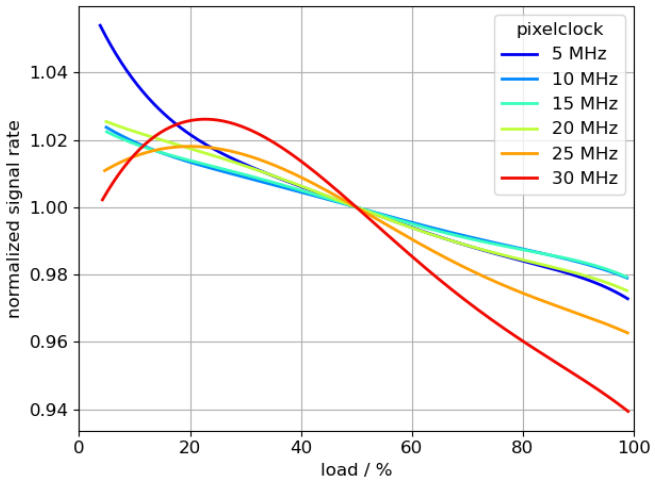

Figure 4 – Dependence of the non-linearity on the internal pixel clock

angle of the non-linearity characteristics. Figure 4 shows the resulting measurements. The camera's default pixel clock frequency is 20 MHz. For the higher clock frequency, the slope starts to decrease, and additional distortions occur at low levels. This argues for the general idea of a dependence on the pixel clock. But for 20 MHz and the lower clock frequencies at 15 MHz and 10 MHz the non-linearity characteristic is nearly linear with the same slope, so there is no significant effect of the clock change. Only at very low pixel clock frequencies of 5 MHz a small increase at low signal occurs. The reason for this is still unclear but it is probably not an increasing smear effect because this is proportional to the readout time and it should have been grown linear with 15 MHz and 10 MHz. At higher levels the general slope stays the same. From this it can be concluded that for the recommended pixel clock frequencies there is no dependence and therefore signal dependent internal slew rates of the AFE are not the reason of the linear non-linearity.

Results from previous internal research indicated, that the non-linearity shows a spectral dependence (Ebeling, 2020).Using LED-based luminance standards of different colour, namely red, green, and blue luminance standards (dominant wavelength 620 nm, 530 nm, and 475 nm, full width at half maximum (FWHM) ≈20…30 nm) instead of one based on an incandescent lamp (illuminant A), revealed that the constant slope of the non-linearity is a systematic effect related to the present spectral distribution. Figure 5 shows the results of these measurements with only small non-linearity for blue light which builds a basic form that gets tilted for green and red light. With this we can state that a spectral dependence is the main reason of what appears as "linear" non-linearity.

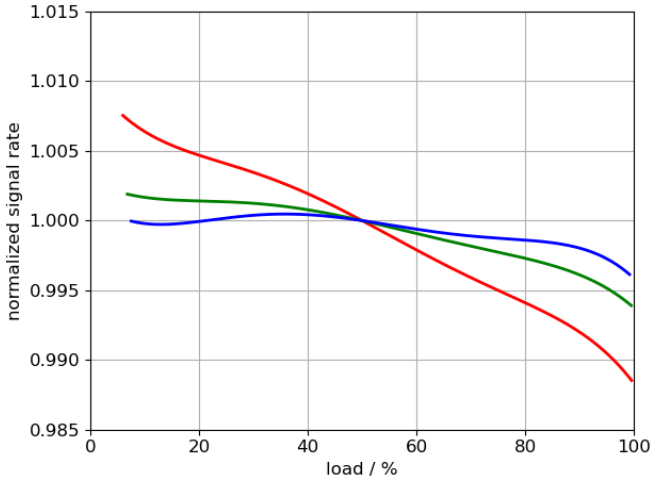

Figure 5 –Non-linearity characteristic for red, green, and blue light

3 Investigation of the spectral dependence

Now we will investigate the spectral dependence in more detail by using a narrow band (~5 nm) optical fibre light source based on a xenon lamp in combination with a monochromator. After dismounting the lens, the tip of the fibre directly irradiates a small region of the sensor. The measurements are carried out in a wavelength range from 350 nm to 1000 nm in steps of 50 nm or 25 nm. Figure 6 shows the resulting non-linearities in a 2D and a 3D plot. For monochromatic irradiation in the range from 350 nm to 500 nm no change of the linear slope occurs, but between 550 nm and 800 nm the linear slope decreases. For wavelengths above 850 nm no further decrease can be seen.

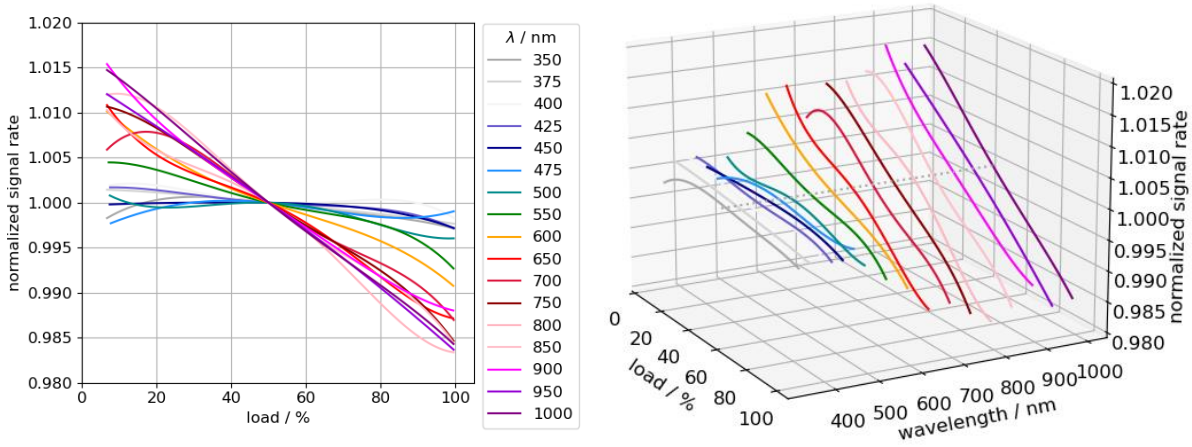

Figure 6 – Spectral dependence of the non-linearity characteristic

In Figure 7 the gradient of the characteristics between 40% and 70% load is shown. This visualizes the dependence of the slope on the wavelength. It drops from about zero below a wavelength of 500 nm to about -3×10^{-4} above 850 nm.

This behaviour can be explained by the combination of two aspects. For semiconductors like silicon, the absorption coefficient of light and therefore the generation rate profile inside the photodiode strongly depends on the wavelength and is in the range of the pixel structure. While the charges accumulate inside the pixel, the extension of the depletion region of the photodiode and thereby of the related drift field is reduced. The charge generation profile from long wavelengths more extensively exceeds the depletion region, resulting in a charge collection rate of

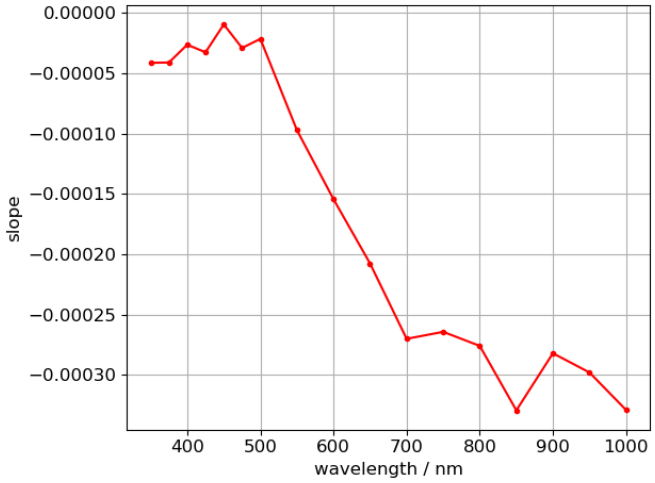

Figure 7 – Slope of the non-linearity polynomials

the photodiode that significantly drops during the integration time. The pixel signal of each measurement (i.e. image) corresponds to the effective, averaged collection rate at the end of the integration time.

It is to emphasize that this effect strongly depends on the internal design of the pixel by means of its electronic structure, namely the doping profile of pixel diode and passivation of surfaces, i.e. of trenches between pixels. The significance of the effect and its wavelength characteristic cannot be transferred between devices of different design. In addition, the effect of spectral dependence needs not to exist for all devices with charge accumulating sensors. E.g. it vanishes in case the depletion region of a pin-diode is not significantly reduced by the accumulated charges or extends the generation profile also for long wavelengths. Figure 8 shows an example of a device without a spectral dependent non-linearity component. Here, the whole non-linearity can be attributed to the analogue signal processing chain.

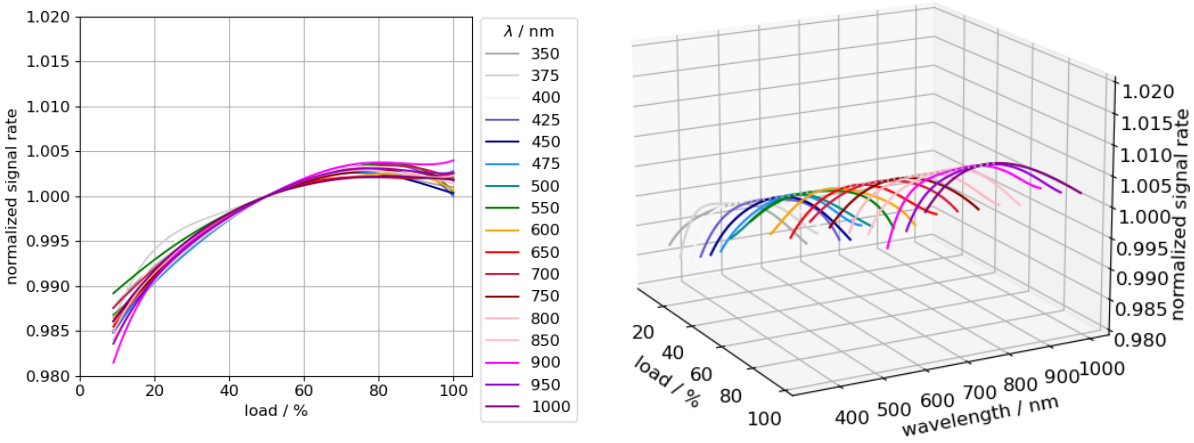

Figure 8 – Example for a non-linearity characteristic without a spectral dependence

For the representative example in of Figure 6 the overall non-linearity consists of two components, the signal-processing chain (visible up to 500 nm) and the spectral dependence that applies above 500 nm. For this camera it is valid to conclude that the spectral dependence dominates the non-linearity characteristic.

A consequence of the spectral dependence of the non-linearity is a distortion of the signal across the image despite a non-linearity correction is applied. For this specific device, which is an ILMD, this can be shown by measurements of the luminance of red, green, blue luminance

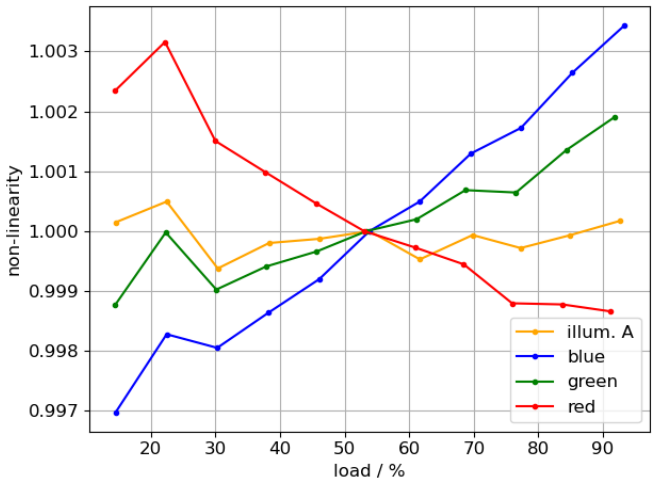

Figure 9 – Non-linearity of the luminance signal of an ILMD (with internal non-linearity correction) for different spectral distributions

standards and one based on an incandescent lamp (illuminant A) with a series of integration times to vary the internal load (signal) value, normalized to the luminance at a load of ≈50%. This is equivalent to the linearity measurements before but renders the internally determined luminance signal, not uncorrected signal values. All internal corrections as implemented and parametrized by the manufacturer are active, namely also a non-linearity correction. With sufficient averaging it could be expected that the luminance value is independent on the integration time and the internal load value. But Figure 9 shows that this only holds for the incandescent source (illuminant A) whose spectral distribution is very similar to the one used for determination of the internal correction parameters. For the other sources we see an over- or under-compensation.

4 Approach on handling spectral non-linearity

Before applying more complex evaluations it should be verified whether a spectral non-linearity exists for a specific device at all. This can be done by determining the non-linearity with a red and a blue light source (in general: narrow-banded sources covering the range of the relevant spectral responsivity) and testing of the signal characteristic for significant difference (see Figure 5) and to check them for a decrease to higher load levels for the red light source.

If it is intended to correct the spectral non-linearity and not just take it as an uncertainty contribution, then the non-linearity of the signal-processing chain and the spectral part need to be determined separately. The analogue signal processing non-linearity can be determined by using blue light for the illumination, with shortest available wavelength within the detection band and therefore largest absorption coefficient and shortest absorption depth (Figure 5, blue curve). This defines the basic non-linearity function that is relevant for all wavelengths.

The offset compensated sensor signal can be modelled as an initial value problem

$$\mathrm{y_{oc}} = \int_0^{t_\mathrm{int}} \int k_\mathrm{conv}(n_\mathrm{e}, \lambda) \cdot E(\lambda) \mathrm{d}\lambda \, \mathrm{d}t \cdot k_\mathrm{sys} \cdot f_\mathrm{NL,sigproc}(\mathrm{y_{oc}}) \tag{4}$$

with the spectral responsivity $k_\mathrm{conv}(n_\mathrm{e}, \lambda)$ of the sensor that additionally depends on the number of charges n_e, converting the spectral pixel irradiance $E(\lambda)$ into charges. The accumulated charges at the end of the integration time then get transformed by an internal system gain k_sys into the output signal $\mathrm{y_{oc}}$. The spectral responsivity $k_\mathrm{conv}(n_\mathrm{e}, \lambda)$ can be split into a constant part at reference load level and a component $f_\mathrm{NL,spectral}$ that models the relative change (spectral non-linearity):

$$\mathrm{y_{oc}} = f_\mathrm{NL,spectral}(\mathrm{y_{oc}}, \lambda_\mathrm{eff}) \cdot t_\mathrm{int} \cdot \int k_\mathrm{conv,ref}(\lambda) \cdot E(\lambda) \, \mathrm{d}\lambda \cdot k_\mathrm{sys} \cdot f_\mathrm{NL,sigproc}(\mathrm{y_{oc}}) \tag{5}$$

The handling of the spectral dependence of $f_\mathrm{NL,spectral}$ would usually require the knowledge of the spectrum of $E(\lambda)$, respectively the source spectrum, to estimate an “effective” wavelength λ_eff at which the effective non-linearity matches the monochromatic one. This is not a feasible approach because the source spectrum is generally not available for all parts of a scene. A solution can be to exploit the simplicity of the spectral dependence of the non-linearity. Recalling how this investigation started we can state that for the presented devices a linear decrease through the reference point (here 50% load) will be an appropriate model. Because this depends on the interaction between depletion zone and charge generation profile inside the pixel we cannot exclude other characteristic functions, e.g. slightly curved ones, but it can be expected to be a simple monotonically decreasing function.

$f_\mathrm{NL,spectral}$ can be determined directly for each region of interest of the image if a set of images with sufficiently different load levels are taken. This approach is based on the idea that is commonly used in HDR algorithms to determine camera response functions (Mitsunaga and Nayar, 1999). The camera response functions in that context are usually strong non-linearities caused by an internal gamma correction. From a series of images with varying integration time and under the prerequisite of a constant scene the combination of all pixel values in the image and integration time allows to reconstruct the response curve. Here we cannot combine the data of multiple regions in the image because the corresponding scene may contain elements of different spectral distributions. But for this simple linear non-linearity function only two data points

with sufficiently large distance at the signal/load scale are required to estimate the effective slope.

5 Example measurement

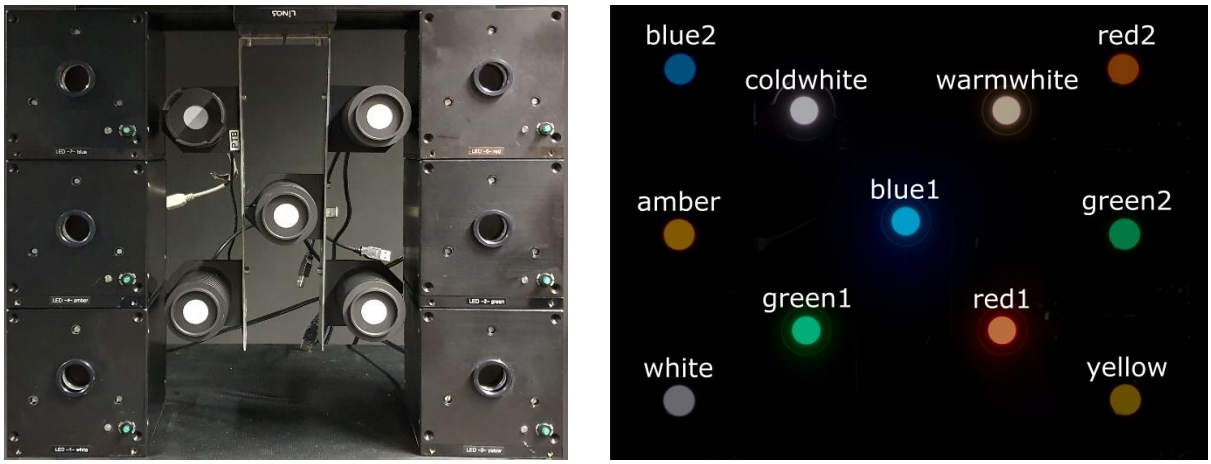

Figure 10 – Exemplary scene based on eleven luminance standards of different colour

To verify the approach an exemplary scene was measured. The scene consists of a set of LED based luminance standard sources with different colour and luminance level, see Figure 10. The analogue signal processing non-linearity $f_{\mathrm{NL,sigproc}}$ originates from the averaged spectral measurements in Figure 7 between 350...500 nm. To rate the combined non-linearity that is to be determined, the overall non-linearities for each source are derived from a high-resolution series regarding the integration time steps. The size of the evaluation regions of each source were 31x31 pixels of the image. These reference non-linearities are shown in Figure 11.

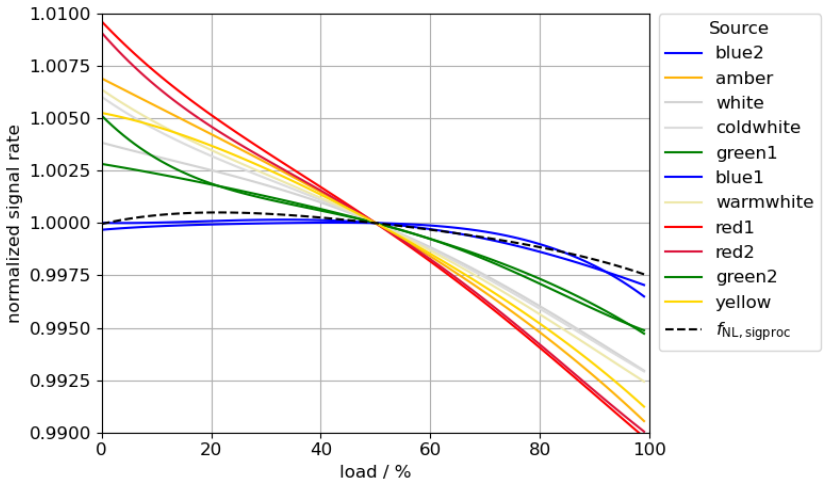

Figure 11 –Reference non-linearities for each source

Then, the data for the estimation of the spectral non-linearity was gathered by a low-resolution series with just enough integration times to collect for each source at least two images with a signal load between 20% and 100%. No pixel of the evaluation region should be in overload (end of the AD-converter range). The 20% limit at the lower end should ensure that the signal is not dominated by noise. In the following evaluation we use only the two images with lowest and highest load level according to above limits.

For the pixels of each region of each selected image

- subtract the ADC-offset: $y_{\mathrm{oc}} = y - y_0$ (6)
- correct the signal-processing non-linearity: $y_{\mathrm{spnlcorr}} = \frac{y_{\mathrm{oc}}}{f_{\mathrm{NL,sigproc}}(y_{\mathrm{oc}})}$ (7)
- calculate the mean value for the evaluation region $\overline{y}_{\mathrm{spnlcorr}}$
- calculate the signal rate by dividing the mean signal value by the integration time:

  $$y_{\mathrm{rate}} = \frac{\overline{y}_{\mathrm{spnlcorr}}}{t_{\mathrm{int}}} \quad (8)$$

- fit a line through all $y_{\mathrm{rate},i}$ of the selected images i. The dependent variable is $y_{\mathrm{rate},i}$ and the independent variable is y_{oc} or, as we use it here, the load level.
- calculate the value of this line at the reference point y_{ref} (here 50% load)
- the estimate for spectral non-linearity $f_{\mathrm{NL,spectral}}(y_{\mathrm{oc}})$ is then given by normalizing the line equation to y_{ref} (divide line coefficients by y_{ref}).

  Figure 12 shows the resulting estimates for the measured regions with selected data points used for the parametrization of the linear slope model. For the blue sources the slopes are slightly positive. This contradicts the model and is attributed to noise.
- correct y_{spnlcorr} for the estimated spectral non-linearity error:

  $$y_{\mathrm{corr}} = \frac{y_{\mathrm{spnlcorr}}}{f_{\mathrm{NL,spectral}}(y_{\mathrm{oc}})} \quad (9)$$

  y_{corr} is the signal including all corrections.

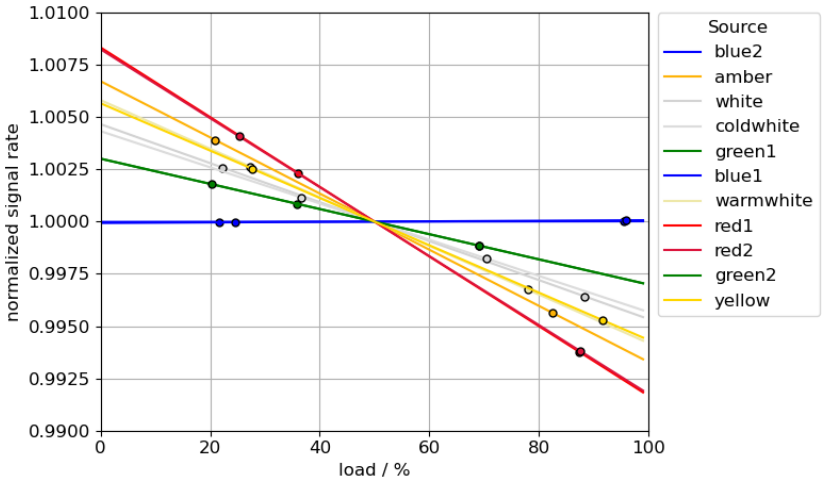

Figure 12 – spectral dependent non-linearity components estimated from a few spot measurements of LED-based luminance standards shown in Figure 10

6 Discussion

To test the quality of this estimation we use the reference non-linearities of Figure 12 and correct for both non-linearity components. Figure 13 shows the results. For an optimal compensation the result should be a horizontal line at 1. The deviations from that line show the residual error. From the small relative residual error below 0.1% for the range above 10% load that is considered to be relevant in well-designed measurements we can conclude that the approach of a region-wise estimation of the spectral component of the non-linearity without knowing the source spectrum generally works.

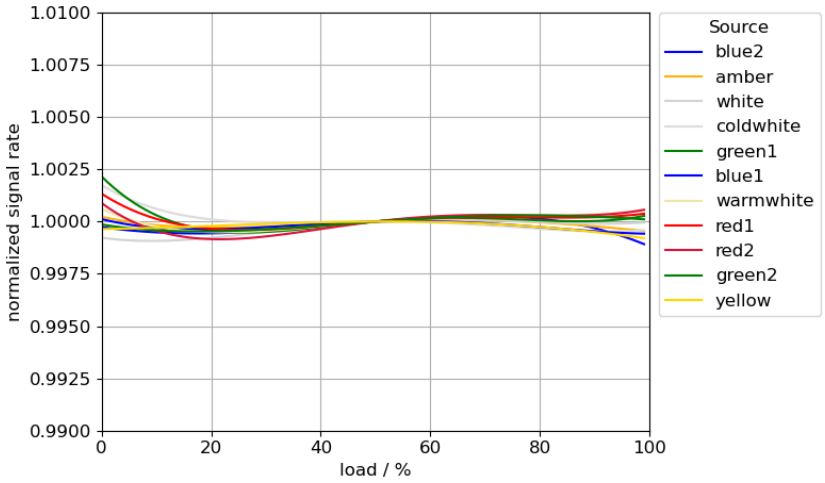

Figure 13 – Residual non-linearities after compensating signal-processing non-linearity and the estimated spectral non-linearity; ideal is a horizontal line at 1

But there are other objectives that still need to be worked on. In the exemplary measurement we selected evaluation regions that led to an averaged measurement value with reduced noise. It would be desirable to be independent of spatial averaging to apply this method pixel-wise (not selecting an evaluation region) but still getting a stable result that is dominated by noise but does not require a lot of temporal averaging by means of multiple images. Also, the forecasting of integration times needed to get a reasonable distribution of measurement points for each pixel needs to be improved. Finally, an uncertainty estimation for the spectral non-linearity function needs to be assigned that can be propagated to the measurement result.

Our results demonstrate that for some pixel detectors the spectral dependent non-linearity is a significant systematic error which emerges in relative evaluations of pixel measurements, namely in case a non-linearity correction and averaging (in the temporal or spatial domain) is employed to reduce noise effects. Compared to the measurement uncertainty of single luminance images this might be neglected as the uncertainty assigned to the luminous responsivity, temperature dependence, or stray-light are more severe.

Acknowledgment

This work was carried out within joint normative research projects (19NRM02 RevStdLED and 21NRM01 HiDyn) which have received funding from the EMPIR programme and from the European Partnership on Metrology, both co-financed by the Participating States and the European Union's Horizon 2020 Research and Innovation Programme.

References

Ebeling, H., 2020. Charakterisierung des Rohsignals von bildgebenden Leuchtdichtemessgeräten (master thesis). Institut für Halbleitertechnik, Technische Universität Braunschweig.

Ferrero, A., Campos, J., Pons, A., 2006. Correction of photoresponse nonuniformity for matrix detectors based on prior compensation for their nonlinear behavior. Appl Opt 45, 2422–2427. https://doi.org/10.1364/AO.45.002422

Mitsunaga, T., Nayar, S.K., 1999. Radiometric Self Calibration, in: 2013 IEEE Conference on Computer Vision and Pattern Recognition. IEEE Computer Society, Los Alamitos, CA, USA, p. 1374. https://doi.org/10.1109/CVPR.1999.786966